Adaptive evolution of threonine deaminase in plant defense against insect herbivores

Eliana Gonzales-Vigil[a], Christopher M. Bianchetti[b,c,d], George N. Phillips, Jr.[b,d], and Gregg A. Howe[a,e,1]

[a]Department of Energy-Plant Research Laboratory, Michigan State University, East Lansing, MI 48824; [b]Department of Biochemistry, University of Wisconsin, Madison, WI 53706; [c]Graduate Program in Biophysics, University of Wisconsin, Madison, WI 53706; [d]Center for Eukaryotic Structural Genomics, University of Wisconsin, Madison, WI 53706; and [e]Department of Biochemistry and Molecular Biology, Michigan State University, East Lansing, MI 48824

Edited by Maarten J. Chrispeels, University of California at San Diego, La Jolla, CA, and approved February 25, 2011 (received for review October 27, 2010)

Gene duplication is a major source of plant chemical diversity that mediates plant–herbivore interactions. There is little direct evidence, however, that novel chemical traits arising from gene duplication reduce herbivory. Higher plants use threonine deaminase (TD) to catalyze the dehydration of threonine (Thr) to α-ketobutyrate and ammonia as the committed step in the biosynthesis of isoleucine (Ile). Cultivated tomato and related *Solanum* species contain a duplicated *TD* paralog (*TD2*) that is coexpressed with a suite of genes involved in herbivore resistance. Analysis of TD2-deficient tomato lines showed that TD2 has a defensive function related to Thr catabolism in the gut of lepidopteran herbivores. During herbivory, the regulatory domain of TD2 is removed by proteolysis to generate a truncated protein (pTD2) that efficiently degrades Thr without being inhibited by Ile. We show that this proteolytic activation step occurs in the gut of lepidopteran but not coleopteran herbivores, and is catalyzed by a chymotrypsin-like protease of insect origin. Analysis of purified recombinant enzymes showed that TD2 is remarkably more resistant to proteolysis and high temperature than the ancestral TD1 isoform. The crystal structure of pTD2 provided evidence that electrostatic interactions constitute a stabilizing feature associated with adaptation of TD2 to the extreme environment of the lepidopteran gut. These findings demonstrate a role for gene duplication in the evolution of a plant defense that targets and co-opts herbivore digestive physiology.

jasmonate | plant–insect interaction | protein stability | induced resistance | molecular evolution

Higher plants have evolved the ability to synthesize an extraordinary range of compounds that contribute to defense against herbivory. A coevolutionary arms race involving iterative cycles of plant adaptation and herbivore counteradaptation is believed to be the driving force in the escalation of phytochemical diversity (1, 2). This theory is supported by the sporadic phylogenetic distribution of defensive metabolites in the plant kingdom, as well as evidence that these compounds are not essential for normal plant growth and development (3). Despite the importance of the arms-race paradigm for explaining plant chemical diversity and plant–herbivore interactions in general, our understanding of the molecular evolution of chemical defensive traits is still in its infancy.

The phytochemical arsenal for deterring herbivores includes low molecular-weight metabolites (so-called secondary metabolites), as well as proteins that exert toxic or antinutritional effects (4, 5). Among the best-studied defensive proteins are wound-inducible proteinase inhibitors (PIs) that form highly stable complexes with insect digestive proteases. Protease inhibition by PIs results in decreased digestion of dietary protein, depletion of essential amino acids, and, consequently, decreased rates of insect growth and development (6). This form of antinutritional defense appears to exploit the low protein content of plant tissue, which is often a limiting factor for the growth of insect herbivores (7). Some plants use additional strategies to reduce amino acid availability. *Solanum lycopersicum* (cultivated tomato) expresses alkaliphilic isoforms of arginase and threonine deaminase (TD) that act in the insect gut to degrade the essential amino acids arginine and threonine, respectively (8). These specialized enzymes provide an attractive opportunity to study the mechanisms and molecular evolution of plant adaption to herbivory.

Threonine deaminase (EC 4.3.1.19) is a pyridoxal phosphate (PLP)-dependent enzyme that converts L-Thr to α-ketobutyrate and ammonia as the committed step in the biosynthesis of Ile. Biosynthetic TDs in plants and bacteria consist of an N-terminal PLP-binding catalytic domain and a C-terminal regulatory domain that is subject to negative feedback inhibition by Ile (9). Many plant species have a single *TD* gene that is essential for Ile synthesis; defects in this gene result in Ile auxotrophy and severely impaired growth and development (10, 11). Tomato and closely related solanaceous plants contain a duplicated *TD* gene (*TD2*) that encodes a novel isoform (51% identical to TD1) whose expression, together with PIs and other defense-related compounds, is tightly regulated by the jasmonate (JA) signaling pathway (12–15). Accumulation of a highly active, truncated form of TD2 (pTD2) in the gut of lepidopteran insects reared on tomato foliage led to the suggestion that TD2 may have a role in insect resistance (8, 13).

Here, we provide transgenic evidence that TD2 confers resistance of tomato to lepidopteran herbivores, and show that postingestive activation (i.e., proteolytic cleavage) of TD2 is catalyzed by a chymotrypsin-like digestive protease in lepidopteran insects. A role for TD2 in postingestive defense was further supported by biochemical studies showing that TD2 is a markedly more stable enzyme than TD1. Comparison of the structure of pTD2 to other TDs suggests that protein stabilization through increased electrostatic interactions allows TD2 to function in the extreme environment of the lepidopteran gut. Our results implicate gene duplication in the evolution of a host plant defense strategy that has co-opted an essential component of insect digestive physiology.

Results

TD2 Enhances Resistance of Tomato to Insect Herbivores. To determine whether TD2 has a role in defense against insect herbivores, we generated stable transgenic lines of tomato that express an antisense *TD2* cDNA under the control of the *Cauliflower mosaic virus* (CaMV) 35S promoter. Two lines (TDAs7 and TDAs15) exhibiting <10% of WT TD2 activity in flowers were identified and used for further analysis (*Materials and Methods*). These lines did not display any obvious morphological or developmental phenotypes related to Ile deficiency and thus were suitable for use in insect-feeding assays. Larvae of the generalist

Author contributions: E.G.-V., C.M.B., G.N.P., and G.A.H. designed research; E.G.-V. and C.M.B. performed research; E.G.-V., C.M.B., G.N.P., and G.A.H. analyzed data; and E.G.-V., C.M.B., G.N.P., and G.A.H. wrote the paper.

The authors declare no conflict of interest.

This article is a PNAS Direct Submission.

Data deposition: The atomic coordinates have been deposited in the Protein Data Bank, www.pdb.org (PDB ID code ID 3IAU).

[1]To whom correspondence should be addressed. E-mail: howeg@msu.edu.

This article contains supporting information online at www.pnas.org/lookup/suppl/doi:10.1073/pnas.1016157108/-/DCSupplemental.

herbivore *Spodoptera exigua* reared on TDAs7 plants for 4 or 7 d were significantly heavier ($P < 0.0001$) than larvae grown on WT plants (Fig. 1*A*). Similar results were obtained for larvae grown for 7 d on the TDAs15 line ($P < 0.005$). Increased *S. exigua* performance on the transgenic lines was correlated with reduced TD2 protein levels in insect-challenged leaves (Fig. 1*B*). Larvae of *Trichoplusia ni*, another lepidopteran herbivore with a broad host range, also gained more weight on TDAs7 plants in comparison with WT (Fig. S1*A*). In contrast, the coleopteran pest *Leptinotarsa decemlineata* (Colorado potato beetle) did not gain more weight on TDAs7 plants relative to the WT host (Fig. S1*B*). These findings establish TD2 as a component of the induced resistance response of tomato to lepidopteran herbivores.

Proteolytic Activation of TD2 by a Chymotrypsin-Like Protease in Lepidopteran Insects. The C-terminal regulatory domain of TD2 is proteolytically cleaved during passage of tomato leaf tissue through the *Manduca sexta* and *T. ni* digestive systems, which allow the enzyme to efficiently metabolize Thr in the presence of high Ile levels in the gut (8, 13). Immunoblot analysis of frass (i.e., feces) collected from *S. exigua* larvae reared on WT plants showed that TD2 is processed in a similar manner in this plant–insect interaction (Fig. S2*A*). Protein digestion in the alkaline midgut of lepidopteran larvae is accomplished mainly by serine proteases, whereas insects from the order Coleoptera have a slightly acidic gut in which cysteine proteases are the major digestive enzymes (16). To determine whether TD2 processing also occurs in coleopteran insects, we compared the extent to which TD2 is cleaved in *M. sexta*, *T. ni*, and *L. decemlineata*. To control for antibody specificity, we also analyzed protein samples collected from each insect species grown on the *jai1* tomato mutant that is defective in JA perception and, as a consequence, does not express TD2 (12). The results show that TD2 is efficiently processed in the two lepidopteran insects but, remarkably, remains intact during passage through *L. decemlineata* (Fig. 2*A*). The absence in *L. decemlineata* frass of intact Rubisco large subunit (RbcL), which is the most abundant soluble protein in tomato leaves, indicates that the lack of TD2 processing cannot be attributed to inefficient digestion of bulk protein. Experiments performed with insects grown on potato plants showed that potato TD2 is also processed in a lepidopteran-specific manner (Fig. S2*B*).

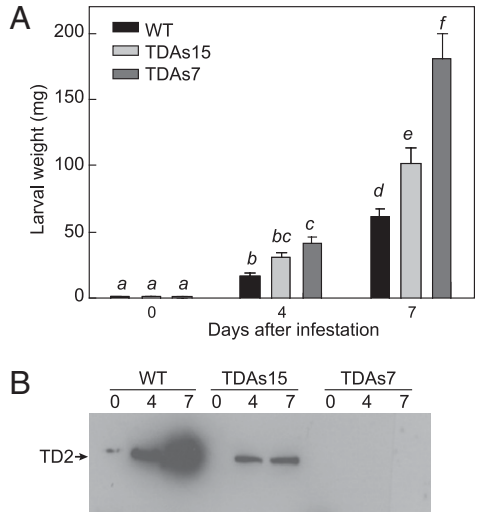

Fig. 1. TD2-deficient tomato lines are compromised in resistance to *S. exigua*. (*A*) Three-day-old *S. exigua* larvae were transferred from an artificial diet to 4-wk-old WT plants or TD2-deficient lines (TDAs15 or TDAs7). One larva was caged per plant. At the indicated time after infestation, larvae were weighed and returned to their plant of origin. Values indicate the mean larval weight ± SE of 18–30 biological replicates. Means with a different italicized letter are significantly different at $P \leq 0.01$. Similar results were obtained in two additional independent bioassays performed with both transgenic lines. (*B*) Western blot analysis of TD2 protein accumulation in undamaged control leaves (0) and damaged leaves from plants that were infested for 4 or 7 d.

Recombinant tomato TD2 was used to determine whether the enzyme could be processed in the lepidopteran gut in the absence of other tomato proteins. Immunoblot analysis of *T. ni* frass protein showed that TD2 added to an artificial diet is completely processed to pTD2 during passage through the insect (Fig. 2*B*). The same experiment performed with *M. sexta* larvae, whose relatively large size facilitated dissection of the gut into its component compartments, showed that dietary TD2 is processed as it moves from the foregut to the midgut (Fig. 2*C*). A crude protein extract prepared from frass of *T. ni* larvae grown on an artificial diet efficiently processed recombinant TD2 under alkaline conditions (pH 9.0) in vitro. Ammonium sulfate precipitation was used to partially purify this activity, which quantitatively converts TD2 to pTD2 (Fig. 2*D* and Fig. S3). The processing activity, referred to hereafter as *T. ni* TD2-processing protease (TPP), was insensitive to inhibitors of aspartic, metallo, cysteine, and amino peptidases, but was impaired by Ser protease inhibitors (Fig. S3*A*). The most effective of these inhibitors was chymostatin, which specifically inhibits chymotrypsin-like proteases (Fig. 2*E*). Consistent with the idea that TD2 is processed by a chymotrypsin-like protease, digestion of TD2 with bovine chymotrypsin generated a major product whose tryptic peptide fingerprint was indistinguishable from that of pTD2 generated with TPP (Fig. S3*B*). Thus, we conclude that TD2 is processed to pTD2 in the lepidopteran gut by a chymotrypsin-like protease of insect origin.

Differential Stability of Tomato TD Isoforms. To investigate the hypothesis that TD2 possess unique biochemical properties that enable it to function in the lepidopteran gut, we compared the activity of purified recombinant TD1 and TD2 under various conditions. TD1 and TD2 metabolized L-Thr with an apparent K_m of 5.7 ± 0.6 and 1.0 ± 0.1 mM, respectively. These levels are comparable to the K_m of pTD2 and other plant TDs (13, 17). The V_{max} and k_{cat} of TD1 were approximately eightfold higher than those for TD2, suggesting that TD1 may be more efficient in catalysis. TD1 (Fig. S4) and TD2 (13) are both active at alkaline pH and strongly inhibited (≥90%) by 1 mM Ile (Fig. S5). Incubation of TD2 with TPP resulted in production of pTD2 and a loss of Ile inhibition, which is indicative of the removal of the regulatory domain (Fig. 3*A* and Fig. S5*A*). Treatment of TD1 with TPP resulted in rapid degradation of the protein (Fig. 3*A*) and complete loss of enzymatic activity (Fig. S5*B*). TD1 and TD2 also showed remarkable differences in temperature sensitivity: TD2 was optimally active at 60 °C, whereas TD1 was maximally active at 16 °C, with no activity detected at temperatures above 55 °C (Fig. 3*B*). Incubation of TD1 at 55 °C for 1 min resulted in complete loss of activity. The same treatment had only a marginal effect on TD2 activity (Fig. 3*C*), demonstrating that protease resistance and thermostability are properties unique to TD2.

Crystal Structure of pTD2. We determined the crystal structure of a recombinant form of pTD2, which, like native pTD2, consists solely of the PLP-binding catalytic domain and the α-helical linker that connects the catalytic and regulatory domains of TD2. The protein crystallized as a tetramer in which each monomer contacts only two other monomers (Fig. 4*A*). The resulting structure gives the overall appearance of a dimer of dimers, as reported for the homologous *Escherichia coli* TD structure (*Ec*TD) and the biodegradative form of TD in *Salmonella typhimurium* (9, 18). Size-exclusion chromatography showed that native pTD2 purified from frass of tomato-reared *M. sexta* has an apparent molecular weight of 143 kDa (Fig. S6), which is in good agreement with the calculated size of the pTD2 tetramer. The pTD2 crystal structure

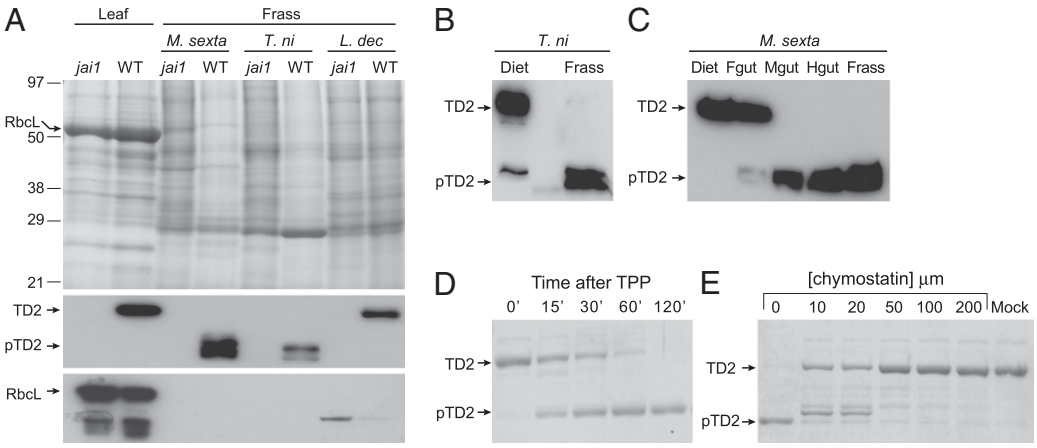

Fig. 2. TD2 is activated by a chymotrypsin-like protease in the lepidopteran midgut. (*A*) Total protein was extracted from tomato leaves that were damaged by *L. decemlineata* (Leaf), or from feces of *M. sexta*, *T. ni*, and *L. decemlineata* larvae reared on wild-type (WT) or *jai1* plants (Frass). Proteins (20 μg) were separated by SDS/PAGE and stained with Coomassie Blue (*Top*). The same samples were used for immunoblot analysis with anti-TD2 (*Middle*) and anti-Rubisco large subunit (RbcL; *Bottom*) antibodies. Arrows denote polypeptides corresponding to RbcL, TD2, and pTD2. (*B*) Fourth-instar *T. ni* larvae were reared for 24 h on an artificial diet containing recombinant TD2, after which insect frass and the remaining diet were collected for protein extraction. Proteins were separated by SDS/PAGE and analyzed by immunoblotting for the presence of TD2. (*C*) *M. sexta* larvae (third instar) were allowed to feed on a TD2-containing diet as described above. Actively feeding larvae were frozen and then dissected. Protein extract prepared from the remaining diet, foregut (Fgut), midgut (Mgut), hindgut (Hgut), and frass were analyzed by immunoblotting for the presence of TD2. (*D*) Coomassie Blue-stained gel showing the TD2 cleavage products generated at various times (min) after incubation of recombinant TD2 with partially purified digestive proteases (TPP) isolated from frass of *T. ni* larvae grown on an artificial diet. (*E*) Dose-dependent effect of chymostatin on TD2 processing by *T. ni* digestive proteases. Chymostatin (at the indicated concentration in micromolar) was incubated with TPP for 15 min before addition of 0.4 μg TD2 substrate. Reactions were incubated at 37 °C for 1 h. Cleavage products were separated by SDS/PAGE, and the resulting gel was stained with Coomassie Blue. A reaction containing TD2 without the *T. ni* protease or chymostatin was included as a control (Mock).

revealed that the helical linker defining the cleavage site of each monomer is positioned at the exterior of the tetramer (Fig. 4*A*) and thus is likely accessible to digestive proteases. The catalytically active portion of pTD2 is composed of two distinct domains (N1 and N2) that adopt similar folds (Fig. S7*A*). The cavity between the two domains contains the Thr-binding active site and PLP cofactor, which is covalently bound through a Schiff-base linkage to the ε-amino group of Lys143 (Fig. S7*B*).

To gain insight into the molecular basis of pTD2 stability, we compared structural features of pTD2 to those of the catalytic domain of *Ec*TD (9) and a TD1 homology model (Table 1). The exposed and buried surface areas for apolar and polar atoms were similar between each of the three proteins, suggesting that hydrophobic effects are not a major determinant of pTD2 stability. Likewise, the amino acid composition and area of the tetramer interface were similar between pTD2 and *Ec*TD. pTD2 showed a slight increase (~10%) in the number of hydrogen bonds in comparison with catalytic regions of *Ec*TD and TD1. More striking, however, the crystal structure of pTD2 revealed a more extensive network of ion pairs, which are known to stabilize the tertiary structure and often correlate with increased protein thermostability (19, 20). The thermophilic pTD2 has five and seven more ion pairs than *Ec*TD and a TD1 homology model, respectively, as defined by oppositely charged groups that interact at a distance of ≤4 Å (Table 1). The pTD2 structure is also characterized by a greater number of critical ion pairs, which are interactions that bridge regions of the protein separated by ≥10 amino acids (19) (Fig. 4*B* and Fig. S8). Seven critical ions pairs observed in the pTD2 structure are not predicted by the TD1 homology model (Fig. 4*B*). Charged residues contributing to three of these critical ion pairs (Asp100-Lys245, Glu116-Arg133, and Glu93-Lys335) are not conserved in TD1 (Fig. S8) and thus are unequivocally unique to pTD2.

Discussion

The growth and development of insect herbivores depends on their ability to acquire essential amino acids by digestion of plant protein. Here, we describe the biochemical and structural features of the defense-related TD2 isoform from tomato that exploits this nutritional vulnerability. TD2 appears to reduce herbivory by acting in the insect gut to degrade Thr, which is an essential and limiting nutrient for the growth of lepidopteran larvae (11). A biochemical function for TD2 in postingestive Thr depletion is supported by the correlation between TD2 abundance in tomato leaves and reduced Thr levels in the insect midgut (8). pTD2 also uses L-Ser as a substrate and thus may affect the availability of this amino acid as well (13). The high reactivity of unionized ammonia, which is generated by pTD2-catalyzed breakdown of amino acids, raises the possibility that pTD2 also exerts toxic effects in the highly alkaline lepidopteran gut.

TD2 has all of the hallmarks of a chemical defensive trait, as predicted by plant–herbivore coevolutionary theory. We demonstrate genetically that TD2 has a role in defense against generalist lepidopteran herbivores but, interestingly, does not protect against the coleopteran insect *L. decemlineata*. As is typical for defensive secondary metabolites, the *TD2* paralog is present in a narrow phylogenetic range of *Solanum* species (13). In contrast to plants that maintain a single essential copy of *TD* (10, 11), tomato does not require TD2 for normal growth and development (ref. 12 and this study). The wound-induced expression of TD2 in leaves is tightly controlled by the JA signaling pathway that orchestrates induced resistance to herbivory (13, 14). Finally, TD2 is expressed at extraordinarily high levels in reproductive tissues (13, 21). This observation is consistent with the notion that plant structures with high fitness values are protected by constitutive defenses (22).

Proteolytic activation of TD2 is catalyzed by a chymotrypsin-like protease of insect origin. Because chymotrypsin has broad substrate specificity and is encoded by a large gene family in the lepidoptera (23), it is likely that multiple chymotrypsins in a given insect species are capable of converting TD2 to pTD2. The dependence of caterpillars on chymotrypsin for food digestion indicates that herbivore adaptation through inhibition of TD2 cleavage is unlikely; co-opting of this essential feature of insect digestive physiology by the host plant may thus be a durable defensive strategy in the chemical arms race for control of amino acid

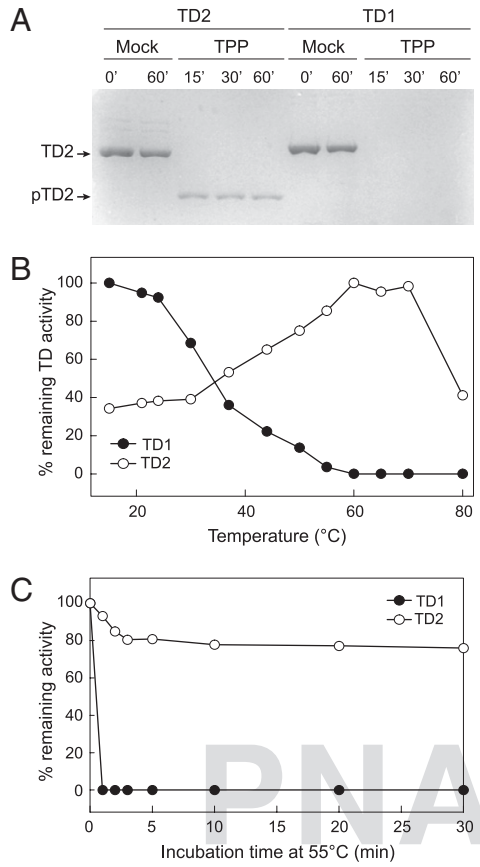

Fig. 3. Differential stability of TD isoforms. (*A*) Recombinant TD2 and TD1 were incubated at 37 °C for the indicated time (min) with partially purified *T. ni* TPP or an equivalent amount of assay buffer (Mock). Reaction products were analyzed by SDS/PAGE and staining with Coomassie Blue. (*B*) Differential temperature optimum of TD1 and TD2. Reaction mixtures containing recombinant TD1 (●) or TD2 (○) were incubated at the indicated temperature for 30 min for the activity assay. Activity levels are expressed relative to the activity observed at the TD1 and TD2 optimal temperature of 16 °C and 60 °C, respectively. (*C*) Differential heat inactivation of TD isoforms. Recombinant proteins were incubated at 55 °C for the indicated time before measuring TD activity at 30 °C. Activity is expressed relative to a control reaction that was not preincubated at 55 °C.

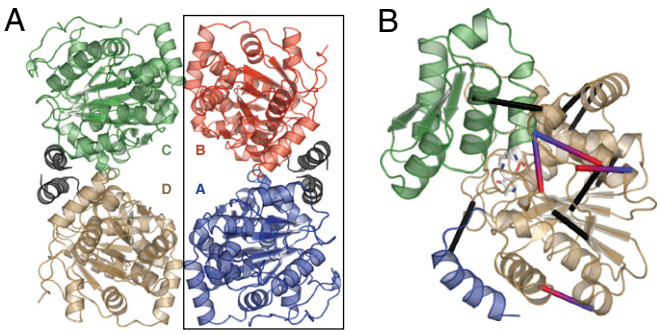

Fig. 4. Crystal structure of pTD2. (*A*) Spatial arrangement of the four monomers (labeled A–D) that compose the pTD2 tetramer, with the helical linker regions that define the TD2 cleavage site shown in black. The box surrounding monomers A and B represents the asymmetric unit. (*B*) Cartoon diagram of pTD2 monomer with N1 domain (brown), N2 domain (green), helical linker (blue), and bound PLP cofactor molecule shown as stick models. Critical ion pairs present in pTD2 but not predicted by the TD1 homology model are shown as black cylinders. Critical ion pairs present in both proteins are shown as cylinders colored in both red (positively charged side chain) and blue (negatively charged side chain).

availability. Colorado potato beetle is reported to contain chymotrypsin-like digestive proteases (24), but nevertheless does not exhibit TD2 processing activity. It is therefore possible that TD2 processing in the lepidopteran gut depends not only on chymotrypsin but also on high pH or other factors that are specific to the lepidopteran gut. The accumulation of tetrameric TD2 in tomato tissues (21) and excretion of tetrameric pTD2 in frass indicates that the protein maintains its multimeric form during passage through the insect, and that the TD2 tetramer is the likely substrate for cleavage by digestive proteases.

In contrast to TD1, TD2 is a remarkably stable protein as determined by enzyme activity at elevated temperature and resistance to digestive proteinases. Increased stability is an important property of defense-related plant proteins that function outside the cell (13). Elucidating the structural features that impart stability is critical to understanding the evolutionary path by which an enzyme in primary metabolism was adapted for a function in defense. A majority of the residues that comprise the pTD2 tetrameric interface are conserved in TD1, which is consistent with the fact that *Ec*TD and TD1 orthologs in other plants also behave as tetramers (9, 17). Thus, although we did not explicitly test the effects of quaternary structure, it is unlikely that tetramer formation is a major determining factor in pTD2 stability. Extensive research has shown that a small increase in the number of ion pairs can account for the difference in stability between thermophilic and mesophilic proteins (19, 25). Given the modest increase in the number of hydrogen bonds and the similarity in the composition of buried surface area, electrostatic interactions of the ion pairs is likely to contribute to increased thermostability of pTD2. The increase in the number of critical ion pairs that bridge distant regions of the protein may be particularly important for maintaining pTD2 in a structurally rigid conformation. Additional studies are needed to assess the role of ionic stabilization in resistance to proteolysis, and to distinguish this hypothesis from the possibility that amino acid substitutions on the surface of pTD2 render the protein resistant to gut proteases. The crystal structure reported here provides a starting point for further studies aimed at elucidating the structural determinants of pTD2 stability.

Gene duplication is a major source of evolutionary innovation in plant chemical diversity (26). However, there is little functional evidence linking gene duplication to plant resistance to herbivory. The conserved intron-exon organization of *TD1* and *TD2*, which are located on chromosomes 10 and 9, respectively, of the *S. lycopersicum* genome (21) (The International Tomato Genome Se-

Table 1. Structural comparison of the catalytic domains of pTD2, *Ec*TD, and tomato TD1

	pTD2*	*Ec*TD†	TD1‡
Length, aa	338	330	337
Hydrogen bonds	379 (1.12/aa)	339 (1.03/aa)	345 (1.03/aa)
Ion pairs	19	14	12
Critical ion pairs	11	9	8
No. of apolar atoms	1,607	1,578	1,611
Buried surface area, Å^2	8,071	7,991	8,005
Exposed surface area, Å^2	2,423	2,425	2,599
No. of polar atoms	909	897	905
Buried surface area, Å^2	4,052	3,770	3,841
Exposed surface area, Å^2	1,662	1,797	1,741
Tetramer interface, Å^2	3,301	3,334	n.d.

n.d., not determined.

*Data based on the crystal structure of pTD2, which comprises residues 78–415 of TD2.

†Data based on the crystal structure of *Ec*TD (9). Only residues 5–334 were used for calculations.

‡Data based on a homology model of TD1. Only residues 88–424 were used for calculations.

quencing Consortium), indicate that *TD2* originated from duplication of an ancestral gene. TD1 and TD2 have maintained the same biochemical activity in Thr catabolism but have diverged markedly with respect to stability, regulatory control of expression, and physiological function. TD2 is thus a striking example of how duplication of genes involved in primary metabolism gives rise to novel defense-related traits. It is likely that selection pressure imposed by lepidopteran herbivores led to this innovation. Interestingly, *Nicotiana attenuata* has a single JA-inducible *TD* gene that serves a dual role in Ile biosynthesis and protection against lepidopteran herbivores (11). This observation raises the possibility that the adaptive role of TD in defense arose before gene duplication and is an example of gene sharing (27, 28). Increasing genome sequence information will help to further elucidate the molecular evolution of TD and other chemical traits that confer plant resistance to herbivory.

Materials and Methods

Plant Material and Transformation. Cultivated tomato [*Solanum lycopersicum*, cultivar (cv.) Micro-Tom] plants were maintained under controlled growth conditions (12). We constructed the *TD2* antisense vector by cloning a PCR-amplified tomato *TD2* cDNA (Table S1) into the XhoI and BamHI sites of the binary vector pBI121 (13, 29). The resulting vector was introduced into *Agrobacterium* strain AGL0 and used to transform tomato (cv. Microtom) cotyledons as previously described (12). Kanamycin-resistant explants were screened by PCR (Table S1) to confirm the presence of the *35S-TD2-As* transgene. Regenerated plants were subsequently screened for reduced TD2 activity levels in flowers, which constitutively express the protein (21). Insect bioassays were conducted with T_3-generation plants obtained from a TDAs7 homozygous line. Alternatively, a PCR screen was used to identify transgene-containing progeny from the TDAs15 line.

Insect Rearing and Bioassays. Insect eggs were obtained from the following sources: *M. sexta*, Department of Entomology, North Carolina State University; *T. ni* and *S. exigua*, Benzon Research; *L. decemlineata*, the Phillip Alampi Beneficial Insect Laboratory, New Jersey Department of Agriculture. The artificial diet for *M. sexta* was obtained from Carolina Biological Supply. Diets for *T. ni* and *S. exigua* were from Southland Products, Inc., with the exception that *T. ni* diet was supplemented with 7 mL/L linseed oil. *S. exigua* was reared on a specified diet for 72 h before transfer of uniformly sized larvae to *TD2* antisense plants. ANOVA was used to test for significant differences in weight among larvae reared on different host genotypes, and larval weight data were ln-transformed to satisfy ANOVA assumptions. The untransformed data were used for constructing Fig. 1*A* and Fig. S1. Differences between treatments were assessed with the least significant difference test. Statistical analysis was performed with SAS software, version 9.1.3. For assays involving feeding of recombinant TD2, *T. ni* and *M. sexta* neonates were grown on an artificial diet (lacking TD2) until they reached the third or fourth instar. Larvae were then starved for 16 h to purge the ingested diet, and then reared for 24 h on a fresh diet containing 0.01% (wt/vol) recombinant TD2. *M. sexta* larvae were frozen at −80 °C for 10 min and then dissected to isolate the foregut, midgut, and hindgut.

Expression and Purification of TD Isoforms. The pET30 vector used previously for expression of *Arabidopsis thaliana* TD (17) was modified by excising the *A. thaliana* cDNA with NdeI and SalI and replacing it with tomato *TD* cDNAs that encode proteins lacking the N-terminal chloroplast-targeting peptide. Before this cloning step, the tomato *TD1* cDNA was subjected to site-directed mutagenesis to remove two NdeI restriction sites in the coding region. This manipulation did not alter the amino acid sequence of TD1. The modified *TD1* cDNA was PCR amplified (Table S1); digested with NdeI and an XhoI; and ligated into the NdeI and SalI sites of pET30. The resulting vector produced a TD1 variant in which the first amino acid (Leu55) of the mature protein is replaced with a new initiator, Met. For expression of pTD2, forward and reverse PCR primers (Table S1) containing NdeI and XhoI sites, respectively, were used to amplify the TD2 coding region corresponding to Lys52–Lys418. Expression and purification of recombinant TD isoforms were performed as described previously (13), except that Ile was added to a final concentration of 1 mM to all buffers (except the final resuspension buffer). The purity of recombinant enzymes as determined by SDS/PAGE was estimated to be above 95%.

TD Enzymatic Assays. TD activity was measured as described previously (8, 13). For determination of kinetic parameters, reactions were performed in triplicate and the data fitted with a nonlinear regression model using Prism 5 for Windows, trial version 5.02 (GraphPad Software). The TD2 processing protease (TPP) was partially purified from *T. ni* frass as follows. Frass (2 g fresh weight) was collected from larvae reared on an artificial diet and frozen at −20 °C until further use. Frozen frass pellets were ground to a fine powder in liquid nitrogen and homogenized in extraction buffer [250 mM Tris-HCl (pH 8.0), 2.5 M NaCl]. Following centrifugation for 30 min at 3,200 × *g*, the supernatant was subjected to three successive rounds of ammonium sulfate precipitation: 0–25% saturation, 25–50% saturation, and 50–75% saturation. Protein precipitated from the 50–75% saturated fraction was resuspended in extraction buffer and dialyzed overnight against 500 vol of extraction buffer at 4 °C. Protein amounts were quantified with a Bradford assay. We performed TD2 cleavage assays by incubating ~0.3 μg TD2 at 37 °C with 0.25 μg TPP in a buffer containing 150 mM Tris-HCl (pH 9.0), 2 mM $CaCl_2$, and 0.5 mM DTT. Reaction products were separated by SDS/PAGE and visualized either by immunoblot analysis with an anti-TD2 antibody (13) or Coomassie Blue staining.

Crystallization, Diffraction Data Collection, and Structure Determination. We used hanging-drop vapor diffusion to grow crystals at 4 °C for data collection. We began by mixing 1 μL of a 10 mg/mL pTD2 solution [5 mM Bis-Tris (pH 7.0), 50 mM NaCl, and 0.3 mM NaN3] with 1 μL reservoir solution [100 mM sodium acetate (pH 4.5), 32% polyethylene glycol 1500, and 100 mM $LiSO_4$]. pTD2 crystals were cryoprotected by the addition of 5% ethylene glycol. X-ray diffraction data were collected at the General Medicine and Cancer Institute Collaborative Access Team (GM/CA-CAT) 23-ID-D beamline at the Advanced Photon Source (APS). Diffraction images were indexed, integrated, and scaled using HKL2000 (30). We performed molecular replacement with MolRep (31) using the biosynthetic form of TD (*Ec*TD) from *E. coli* (PDB ID code 1TDJ) (9). The structure was completed with manual model building in Coot (32) and refinement in Phenix (33). Pertinent information on the structure solution is summarized in Table S2. Model quality was assessed using MolProbity (34). Figures were generated using the PyMOL Molecular Graphics System, version 1.2r3pre (Schrödinger, LLC).

The TD1 homology model was generated using the default parameters of SWISS-MODEL (35) (http://swissmodel.expasy.org/). pTD2 and *Ec*TD were used as the basis for constructing the TD1 model. To determine the total number of hydrogen bonds, we used the WHAT IF optimal hydrogen bonding network Web server (36). Hydrogen bonds were reported if the donor and acceptor were within 3.2 Å. If the charged atoms of two oppositely charged residues were within 4 Å, the interaction was considered an ion pair. The carboxylic O atoms of Asp and Glu were considered negatively charged, and the amino N atoms of Arg, Lys, and His were considered positively charged. The total number of ion pairs was calculated using the Protein Structure Analysis Package (PSAP) (37). Polar and apolar exposed and buried surface areas were calculated with WHAT IF using a probe radius of 1.4 Å (38). C and S atoms were considered apolar, whereas N and O atoms were considered polar. The amount of buried surface area due to tetramerization was calculated using the Protein Interfaces, Surfaces and Assemblies service (PISA) (39).

ACKNOWLEDGMENTS. We are grateful to Christopher Bergum for technical assistance, Hui Chen for estimating the molecular weight of native pTD2, Renaud Dumas for providing the pET30-AtTD vector, and Mark Rausher for helpful discussions during the course of this work. We also thank Marco Herde for assistance with bioassays and Zsofia Szendrei for supplying *L. decemlineata* eggs. This research was supported by US Department of Agriculture Grant 2007-35604-1779 (to G.A.H.); US Department of Energy (Chemical Sciences, Geosciences and Biosciences Division, Office of Basic Energy Sciences, Office of Science) Grants DE-FG02-91ER20021 (to G.A.H.) and DE-FC02-07ER64494 (to G.N.P.); and National Institutes of Health Grant U54 GM074901 (to G.N.P.). Use of the Advanced Photon Source was supported by US Department of Energy, Office of Science, Office of Basic Energy Sciences Contract DE-AC02-06CH11357. The General Medicine and Cancer Institutes Collaborative Access Team (GM/CA-CAT) was funded by National Cancer Institute Grant Y1-CO-1020 and National Institute of General Medical Science Grant Y1-GM-1104.

1. Ehrlich PR, Raven PH (1964) Butterflies and plants: A study in coevolution. *Evolution* 18:586–608.
2. Berenbaum MR, Zangerl AR (2008) Facing the future of plant-insect interaction research: Le retour à la "raison d'être". *Plant Physiol* 146:804–811.
3. Fraenkel GS (1959) The raison d'être of secondary plant substances; these odd chemicals arose as a means of protecting plants from insects and now guide insects to food. *Science* 129:1466–1470.
4. Howe GA, Jander G (2008) Plant immunity to insect herbivores. *Annu Rev Plant Biol* 59:41–66.

5. Zhu-Salzman K, Luthe DS, Felton GW (2008) Arthropod-inducible proteins: Broad spectrum defenses against multiple herbivores. *Plant Physiol* 146:852–858.
6. Ryan CA (1990) Protease inhibitors in plants: Genes for improving defenses against insects and pathogens. *Annu Rev Phytopathol* 28:425–449.
7. Mattson WJ (1980) Herbivory in relation to plant nitrogen content. *Annu Rev Ecol Syst* 11:119–161.
8. Chen H, Wilkerson CG, Kuchar JA, Phinney BS, Howe GA (2005) Jasmonate-inducible plant enzymes degrade essential amino acids in the herbivore midgut. *Proc Natl Acad Sci USA* 102:19237–19242.
9. Gallagher DT, et al. (1998) Structure and control of pyridoxal phosphate dependent allosteric threonine deaminase. *Structure* 6:465–475.
10. Sidorov V, Menczel L, Maliga P (1981) Isoleucine-requiring *Nicotiana* plant deficient in threonine deaminase. *Nature* 294:87–88.
11. Kang JH, Wang L, Giri A, Baldwin IT (2006) Silencing threonine deaminase and JAR4 in *Nicotiana attenuata* impairs jasmonic acid-isoleucine-mediated defenses against *Manduca sexta*. *Plant Cell* 18:3303–3320.
12. Li L, et al. (2004) The tomato homolog of CORONATINE-INSENSITIVE1 is required for the maternal control of seed maturation, jasmonate-signaled defense responses, and glandular trichome development. *Plant Cell* 16:126–143.
13. Chen H, Gonzales-Vigil E, Wilkerson CG, Howe GA (2007) Stability of plant defense proteins in the gut of insect herbivores. *Plant Physiol* 143:1954–1967.
14. Hildmann T, et al. (1992) General roles of abscisic and jasmonic acids in gene activation as a result of mechanical wounding. *Plant Cell* 4:1157–1170.
15. Samach A, Broday L, Hareven D, Lifschitz E (1995) Expression of an amino acid biosynthesis gene in tomato flowers: Developmental upregulation and MeJa response are parenchyma-specific and mutually compatible. *Plant J* 8:391–406.
16. Bolter C, Jongsma MA (1997) The adaptation of insects to plant protease inhibitors. *J Insect Physiol* 43:885–895.
17. Wessel PM, Graciet E, Douce R, Dumas R (2000) Evidence for two distinct effector-binding sites in threonine deaminase by site-directed mutagenesis, kinetic, and binding experiments. *Biochemistry* 39:15136–15143.
18. Simanshu DK, Savithri HS, Murthy MRN (2006) Crystal structures of *Salmonella typhimurium* biodegradative threonine deaminase and its complex with CMP provide structural insights into ligand-induced oligomerization and enzyme activation. *J Biol Chem* 281:39630–39641.
19. Bae E, Phillips GN, Jr (2004) Structures and analysis of highly homologous psychrophilic, mesophilic, and thermophilic adenylate kinases. *J Biol Chem* 279:28202–28208.
20. Szilágyi A, Závodszky P (2000) Structural differences between mesophilic, moderately thermophilic and extremely thermophilic protein subunits: Results of a comprehensive survey. *Structure* 8:493–504.
21. Samach A, Hareven D, Gutfinger T, Ken-Dror S, Lifschitz E (1991) Biosynthetic threonine deaminase gene of tomato: Isolation, structure, and upregulation in floral organs. *Proc Natl Acad Sci USA* 88:2678–2682.
22. Zangerl AR, Rutledge CE (1996) The probability of attack and patterns of constitutive and induced defense: A test of optimal defense theory. *Am Nat* 147:599–608.
23. Srinivasan A, Giri AP, Gupta VS (2006) Structural and functional diversities in lepidopteran serine proteases. *Cell Mol Biol Lett* 11:132–154.
24. Novillo C, Castanera P, Ortego F (1997) Characterization and distribution of chymotrypsin-like and other digestive proteases in Colorado potato beetle larvae. *Arch Insect Biochem Physiol* 36:181–201.
25. Vieille C, Zeikus GJ (2001) Hyperthermophilic enzymes: Sources, uses, and molecular mechanisms for thermostability. *Microbiol Mol Biol Rev* 65:1–43.
26. Ober D (2010) Gene duplications and the time thereafter—examples from plant secondary metabolism. *Plant Biol (Stuttg)* 12:570–577.
27. Des Marais DL, Rausher MD (2008) Escape from adaptive conflict after duplication in an anthocyanin pathway gene. *Nature* 454:762–765.
28. Soskine M, Tawfik DS (2010) Mutational effects and the evolution of new protein functions. *Nat Rev Genet* 11:572–582.
29. Schilmiller AL, Koo AJK, Howe GA (2007) Functional diversification of acyl-coenzyme A oxidases in jasmonic acid biosynthesis and action. *Plant Physiol* 143:812–824.
30. Otwinowski Z, Minor W (1997) Processing of X-ray diffraction data collected in oscillation mode. *Methods Enzymol* 276:307–326.
31. Vagin A, Teplyakov A (1997) MOLREP: An automated program for molecular replacement. *J Appl Cryst* 30:1022–1025.
32. Emsley P, Cowtan K (2004) Coot: Model-building tools for molecular graphics. *Acta Crystallogr D Biol Crystallogr* 60:2126–2132.
33. Adams PD, et al. (2002) PHENIX: Building new software for automated crystallographic structure determination. *Acta Crystallogr D Biol Crystallogr* 58: 1948–1954.
34. Lovell SC, et al. (2003) Structure validation by Calpha geometry: Phi, psi and Cbeta deviation. *Proteins* 50:437–450.
35. Arnold K, Bordoli L, Kopp J, Schwede T (2006) The SWISS-MODEL workspace: A web-based environment for protein structure homology modelling. *Bioinformatics* 22: 195–201.
36. Hooft RWW, Sander C, Vriend G (1996) Positioning hydrogen atoms by optimizing hydrogen-bond networks in protein structures. *Proteins* 26:363–376.
37. Balamurugan B, et al. (2007) PSAP: Protein structure analysis package. *J Appl Cryst* 40: 773–777.
38. Vriend G (1990) WHAT IF: A molecular modeling and drug design program. *J Mol Graphics* 8:52–56.
39. Krissinel E, Henrick K (2007) Inference of macromolecular assemblies from crystalline state. *J Mol Biol* 372:774–797.